

# Research of Ring MEMS Rate Integrating Gyroscopes

Hui Liu, and Haiyang Quan

**Abstract**—This paper To get the angle value with a MEMS rate gyroscope in some specific field, the usual method is to make an integral operation to the rate output, which will lead the error cumulating effect. So the rate gyro is not suitable. MEMS rate integrating gyroscope (MRIG) will solve this problem. A DSP system has been developed to implement the control arithmetic. The system can measure the angle of rotation directly by the control loops that make the sensor work in whole-angle mode. Modeling the system with MATLAB, desirable results of angle outputs are got, which prove the feasibility of the control arithmetic.

**Keywords**—Rate gyroscope, Rate integrating gyroscope, Whole angle mode, MATLAB modeling, DSP control.

## I. INTRODUCTION

MEMS vibratory gyroscopes have received increased attention from automotive and consumer electronics industries in the past decade. However, most commercial MEMS gyroscopes are angular rate measuring sensors employing energy transfer between the drive and the sense mode. These kinds of gyroscopes have obvious advantages in bulk, weight and power and they often have lower price while the performance is eligible. MEMS vibratory gyroscopes can be classified into two broad types, rate gyroscope, measuring rotating rate of the system and rate integrating gyroscope, measuring the absolute angle of rotation [1]. All the vibratory gyroscopes are based on Coriolis effect, that exploit energy transfer between the vibration modes.

There are many kinds of physical structures of gyroscope sensors, one of which is the ring sensor, shown in Fig. 1. The isotropy structure of the ring sensor [2], [3] can effectively weaken the coupling between different modes, so the matching is much easier. The inherent resonant frequency is usually more than 10k Hz, which makes the rigidity more than ten times better comparing with other structures. As a result, this kind of gyroscope will suffer less effect like temperature, acceleration, vibratory, impact and many other effects from environment.

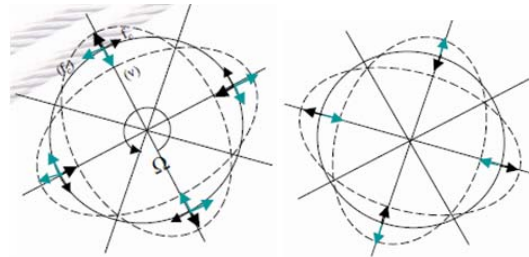


Fig. 1 Two modes of a ring rate gyroscope

Almost all the MEMS vibratory gyroscopes are rate gyroscopes so far. Benefiting from the fact that the control arithmetic of these gyroscopes are simple relatively, and can get the rotating rate, they are being studied and applied diffusely. Most MEMS rate gyroscopes have the performance of rate grade, but only a few labs can reach tactics grade or higher. However, under some specific application, like high dynamic environment, range and scale factor are the most two important parameters. The two parameters are restricted for rate gyroscopes. Many factors like electrode size and spacing, first mode amplitude, ring voltage and driving voltage limit the range, and gain of LNA and front end analog circuits, AD transfer reference voltage will lead to an error in scale factor.

$$SF = \frac{V_{out}}{\Omega} = \frac{2k\omega_n Y_{ref}}{Y_1 \beta_2} = \frac{4k\omega_n V_{AGC} d^4 C_f}{c(\epsilon A V_{HT})^2} \quad (1)$$

All of the imperfections are destructive in high dynamic environment. In actual application when the angle information is needed, the usual method is to make an integral operation to the rate output, which will lead the error cumulating effect. As is shown in Fig. 2, Bias Drift, ARW, and the stability of SF will be integrated to angle output, and cumulate the error.

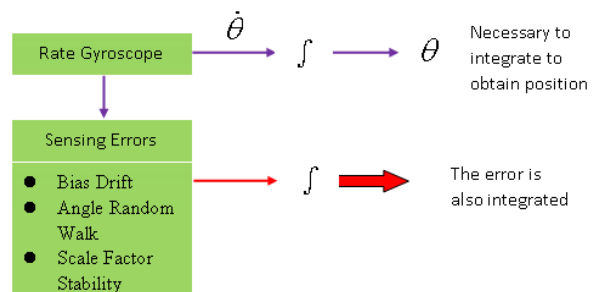


Fig. 2 Error cumulating in integrating

Hui Liu is with the Beijing Microelectronics Technology Institute, P.R. China, (phone: 010-67968115-8317; fax: 010-68757706; e-mail: wukonglyy@gmail.com).

Haiyang Quan is with the Beijing Microelectronics Technology Institute, P.R. China.

MEMS Rate Integrating Gyroscope (MRIG) [4], [5] will solve these programs. This kind of gyroscopes can directly measure the rotating angle of an object, without producing errors from both circuits and mechanical structure after integration. MRIG have very high precision of angle gain factor, that promise wonderful performance of scale factor (<1ppm), and their characteristic of freely precession make their range unlimited. All the advantages provide very expansive application for MRIG.

## II. PRINCIPLES

All MRIG can be simplified to a 2-dof mass-spring system, in which there are two principal directions (normal mode axes) along which the system's natural frequencies are slightly different (shown in Fig. 3 (a)). One of the main error sources in vibratory gyroscopes arises from the mismatch in natural frequencies of the two vibration modes utilized. The analysis of the system can be applied to all MRIG.

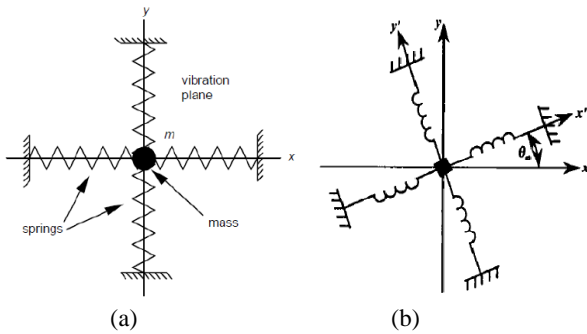


Fig. 3 2-dof vibrating model

### A. Equations of Motion of Generalized Vibratory Gyro

The model above-mentioned is a mass vibrating in x-y plane restricted by axisymmetric linear springs. In the rotating frame, the x-y plane is rotating about the z axis with angular velocity  $\Omega$ , as is shown in Fig. 3 (b). From Newton second law  $F = ma = m\ddot{r}$ , we can get the equations of motion are

$$\begin{aligned} \frac{F_x}{m} &= \ddot{x} - 2\Omega\dot{y} - \dot{\Omega}y + (\omega_2^2 - \Omega^2)x = f'_x \\ \frac{F_y}{m} &= \ddot{y} + 2\Omega\dot{x} + \dot{\Omega}x + (\omega_1^2 - \Omega^2)y = f'_y \end{aligned} \quad (2)$$

Equations (2) contain Coriolis Effect, angle acceleration term and centrifugal force term. The components  $\vec{r}$  and  $\vec{f}$  along the x-y and the x'-y' axis sets are related by the orthogonal transformation equations (3)

$$\begin{aligned} x &= x' \cos \theta - y' \sin \theta \\ y &= y' \cos \theta + x' \sin \theta \end{aligned} \quad (3)$$

Then we can write the equations of motion in terms of x-y components in the form [6].

$$\begin{aligned} \ddot{x} - 2\Omega\dot{y} - \dot{\Omega}y + \left(\frac{\omega_1^2 + \omega_2^2}{2} - \Omega^2\right)x - \frac{\omega_1^2 - \omega_2^2}{2} \\ (x \cos 2\theta_\omega + y \sin 2\theta_\omega) &= f_x \\ \ddot{y} + 2\Omega\dot{x} + \dot{\Omega}x + \left(\frac{\omega_1^2 + \omega_2^2}{2} - \Omega^2\right)y + \frac{\omega_1^2 - \omega_2^2}{2} \\ (y \cos 2\theta_\omega - x \sin 2\theta_\omega) &= f_y \end{aligned} \quad (4)$$

In order to make the equations more intact, angle gain factor k and acceleration factor k' are introduced. If we include linear damping with principal-axis time constants  $\tau_1, \tau_2$ , the generic equations are

$$\begin{aligned} \ddot{x} - k(2\Omega\dot{y} + \dot{\Omega}y) + \frac{2}{\tau} \dot{x} + \Delta\left(\frac{1}{\tau}\right)(\dot{x} \cos 2\theta_\tau + \dot{y} \sin 2\theta_\tau) \\ + (\omega^2 - k'\Omega^2)x - \omega\Delta\omega(x \cos 2\theta_\omega + y \sin 2\theta_\omega) &= f_x \\ \ddot{y} + k(2\Omega\dot{x} + \dot{\Omega}x) + \frac{2}{\tau} \dot{y} - \Delta\left(\frac{1}{\tau}\right)(\dot{y} \cos 2\theta_\tau - \dot{x} \sin 2\theta_\tau) \\ + (\omega^2 - k'\Omega^2)y + \omega\Delta\omega(y \cos 2\theta_\omega - x \sin 2\theta_\omega) &= f_y \end{aligned} \quad (5)$$

In which  $\theta_\tau$  is the azimuth of the  $\tau_1$  principal axis ( $\theta_\omega$  is the azimuth of the  $\tau_2$  principal axis), and (6) are the approximate conditions

$$\begin{aligned} \omega^2 &= \frac{\omega_1^2 + \omega_2^2}{2} & \frac{1}{\tau} &= \frac{1}{2} \left( \frac{1}{\tau_1} + \frac{1}{\tau_2} \right) \\ \omega\Delta\omega &= \frac{\omega_1^2 - \omega_2^2}{2} & \Delta\left(\frac{1}{\tau}\right) &= \frac{1}{\tau_1} - \frac{1}{\tau_2} \end{aligned} \quad (6)$$

We call the equations (5) the equations of motion of the Generic Vibratory Gyroscope [7], [8].

### B. Simplifying Model for MRIG

All tables and figures you insert in your document are only to help you gauge the size of your paper, for the convenience of the referees, and to make it easy for you to distribute preprints.

To implement a MRIG, the 2-dof freely vibrating system should approach the ideal condition. Consequently, we can simplify the model when solving the equations above. Assuming that the two normal-mode frequencies are identical, and there is no damping, no rate input, no external forcing, the equations (5) reduce to

$$\begin{aligned} \ddot{x} + \omega^2 x &= 0 \\ \ddot{y} + \omega^2 y &= 0 \end{aligned} \quad (7)$$

The most general solution to equations (7) can be written in the form.

$$\begin{aligned} x &= a \cos \theta \cos(\omega t + \phi') - q \sin \theta \sin(\omega t + \phi') \\ y &= a \sin \theta \cos(\omega t + \phi') + q \cos \theta \sin(\omega t + \phi') \end{aligned} \quad (8)$$

Equations (8) represent a fact that the trajectory of an ideal 2-dof system is a stationary elliptical orbit described by four parameters  $a, q, \theta, \phi'$ , shown in Fig. 4.

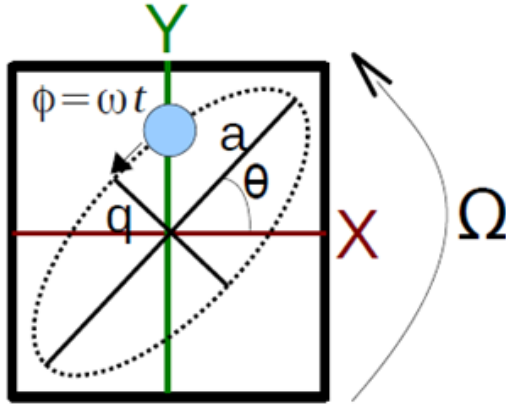


Fig. 4 Equivalent elliptical orbit

When there is no damping and external forcing, the orbit of the ideal 2-dof system will keep its intrinsic shape and precess accordingly following the rotating frame. In a fixed period of time, the azimuth of this orbit relative to the system above is proportional to the azimuth to inertial frame with a coefficient  $k$ . In non ideal environments, the parameters  $a, q, \theta, \phi'$  will be varying along with time because of frequency gap, damping and external forcing etc. However, for any actual MRIG, this kind of varying is slow on a time scale whose unit is  $2\pi / \omega$ .

The analyses above provide appropriate basic principle for the Implementation of MRIG.

### III. CONTROL SCHEME

The basic control problems to MRIG are to maintain the amplitude  $a$  to a prescribed value and to null the quadrature amplitude  $q$ .

However, in the sensor of ring structure, the vibration is in the form of standing wave, which is precessing along with the inertial frame (Fig. 5) rather than fixed on the driving electrodes in rate gyroscope. As a result, the control scheme of MRIG is rather different.

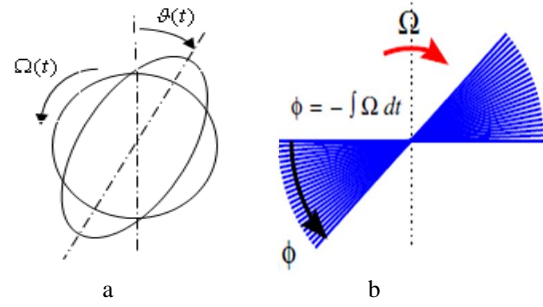


Fig. 5 The precessing of a ring sensor MRIG

Demodulating the signals of the two normal-mode axes, we can get four pickoff demodulated quantities  $c_x, s_x, c_y, s_y$ , which are the basic of all the following signal processing work. The relationship of transforming between orbit parameters  $a, q, \theta, \phi'$  and  $c_x, s_x, c_y, s_y$ , is different in different working pattern. For whole angle mode, there are

$$\begin{aligned} a^2 + q^2 &= c_x^2 + s_x^2 + c_y^2 + s_y^2 \\ a \times q &= c_x s_y - c_y s_x \\ \theta &= 1/2 \arctan \frac{2(c_x c_y + s_x s_y)}{c_x^2 + s_x^2 - c_y^2 - s_y^2} \\ \phi - \phi' &= 1/2 \arcsin \frac{2(c_x s_x + c_y s_y)}{\sqrt{4(c_x c_y + s_x s_y)^2 + (c_x^2 + s_x^2 - c_y^2 - s_y^2)^2}} \end{aligned} \quad (9)$$

The equations above are the basic principle for signal processing part of control system. From (9) we know that three closed loops can stabilize the whole system.

Model the system [9] using MATLAB, the block diagram is shown in Fig. 6.

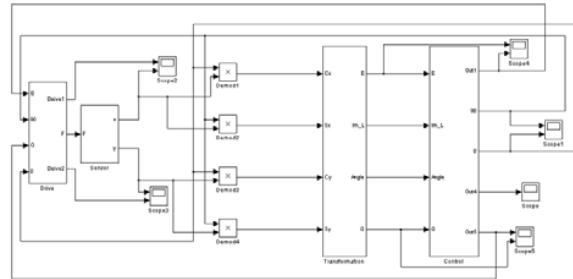
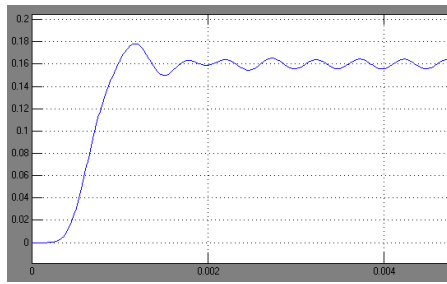


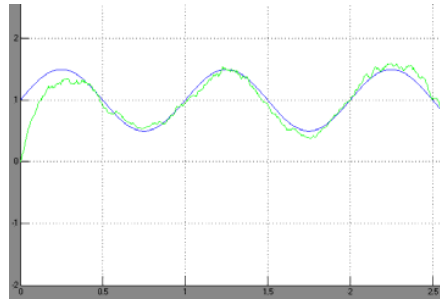
Fig. 6 modeling of MRIG with simulink

The several main parts of the system is the sensor module, demodulation module, angle calculation module, control module and drive module.

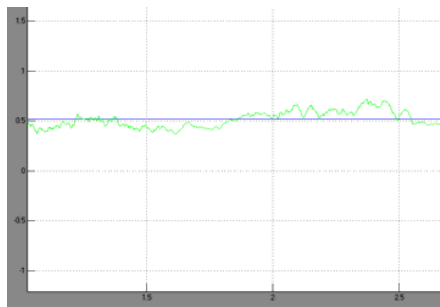
Simulating the system, we get the results of the important modules, which are shown in Fig. 7.



(a) The AGC model



(b) The PID model for tracing



(c) The angle measuring model

Fig. 7 simulation results with MATLAB

The results indicate that, the control algorithm above can implement the angle measuring function, and make the sensor work as rate integrating gyroscopes.

#### IV. CONTROL SYSTEM BASED ON DSP

The main work of the signal processing part is to accomplish the feedback loops, filters and other compensating arithmetic.

Parameter extraction is a proper method to the drive loops. Here we introduce a concept, static energy, denoted by  $E$  ( $E = a^2 + q^2$ ), which is one of the invariants under a transformation corresponding to a rotation pickoff axis set about the  $z$  axis. By using static energy  $E$  as the error variable of PID controller, we can effectively solve the problem how to maintain the vibration amplitude when the stand wave is precessing.

The whole system [10] is described in Fig. 8. First the sensing signals are processed in DSP from the sensor via ADC, and then the driving signals created by closed loops are sent back to the driving electrodes after digital processing via DAC. In Fig. 6,

the function of the transformation block is to transform the demodulation quantities  $C_x, S_x, C_y, S_y$ , to the error variables of the controllers.

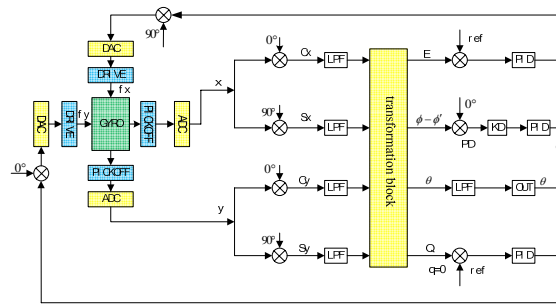


Fig. 8 Whole control scheme of MRIG

#### V. HARDWARE CONNECTION

The control configuration can be divided into three parts. They are analog interface, signal pretreatment circuits and digital processing module.

The analog interface comprises four LNA and C-V convertors, which transform the signal to voltage from capacitance. The signal pretreatment circuits include amplifier, filter, A/D convertor and D/A convertor chips, and the function is to sense the weak voltage and transform them to digital signals. The whole digital processing module is accomplished by DSP chip, implementing all the feedback loops and other compensating arithmetic. The structure frame is shown in Fig. 9.

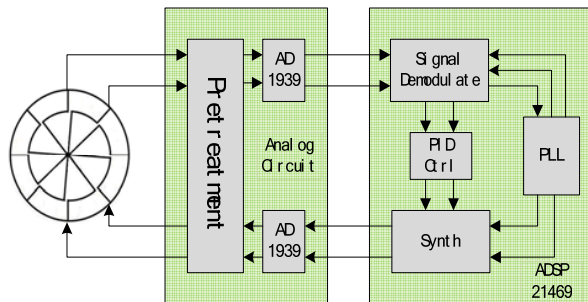


Fig. 9 Hardware platform of MRIG

The signal generation and response signal sampling were based on a codec IC AD1939, which has 8 channels ADC of 24 bit resolution and 192 kHz sampling rate. By employing an internal digital reconstruction filter and an extended sine wave lookup table, the system can create 4 channels of high quality sine wave up to 70 kHz with a frequency resolution of 0.01 Hz. Data transfer between the codec and DSP, and relevant demodulation and control calculation was interrupt driven with sample based processing at a frequency of 192 kHz.

The DSP board has a very high speed core of ADSP-21469, with instruction execution time of 0.2 ns. Employing a hardware circular buffer, addressing all the calculations for signal

generation and measurement such as demodulation and low pass filtering can be completed within 5 $\mu$ s.

#### REFERENCES

- [1] A. M. Shelk, "Type I and type II Micromachined Vibratory Gyroscopes".
- [2] Michael William Putty, "A Micro Machined Vibrating Ring Gyroscope".
- [3] E. J. Loper and D. Lynch, "Vibratory Rotation Sensor", Aug. 28, 1990, U.S. Patent 4,951,508.
- [4] I. P. Prikhodko, S. A. Zotov, A. A. Trusov, A. M. Shkel, "Foucault pendulum on a chip: Rate integrating silicon MEMS gyroscope", *Sensors and Actuators A* 177 (2012) 67- 78.
- [5] J. Cho, J. A. Gregory and K. Najafi, "Single-Crystal-Silicon Vibratory Cylindrical Rate Integrating Gyroscope (CING)", *Transducers* 11, Beijing, China, June 5-9, 2011.
- [6] B. J. Gallacher, "Principles of a Micro-Rate Integrating Ring Gyroscope", *IEEE Transaction on aerospace and electronic systems* VOL. 48, NO. 1 January 2012.
- [7] D.D. Lynch, "Vibratory gyroscope analysis by the method of averaging", 2nd St. Petersburg Int. Conf. on Gyroscopic Technology and Navigation, St. Petersburg, Russia, 1995.
- [8] Z. X. Hu, B. J. Gallacher, J. S. Burdess, C. P. Fell, K. Townsend, "A Parametrically amplified MEMS rate gyroscope", *Sensors and Actuators A* 167 (2011) 249-260.
- [9] C. Painter and A. Shkel, "Experimental evaluation of a control system for an absolute angle measuring micromachined gyroscope", 4th IEEE Conference on Sensors, Oct. 31-Nov. 03, 2005.
- [10] J. A. Gregory, J. Cho, K. Najafi, "MEMS rate and rate-integrating gyroscope control with commercial software defined radio hardware", *IEEE Transducers* 2011, Beijing, China, 2011.